Sensory Processing in the Drosophila Antennal Lobe Increases the Reliability and Separability of Ensemble Odor Representations

Vikas Bhandawat, Shawn R. Olsen, Nathan W. Gouwens, Michelle L. Schlief, and Rachel I. Wilson

Supplementary Online Material

Supplementary Figure 1: Electrophysiological recordings from *Drosophila* olfactory receptor neurons and projection neurons.

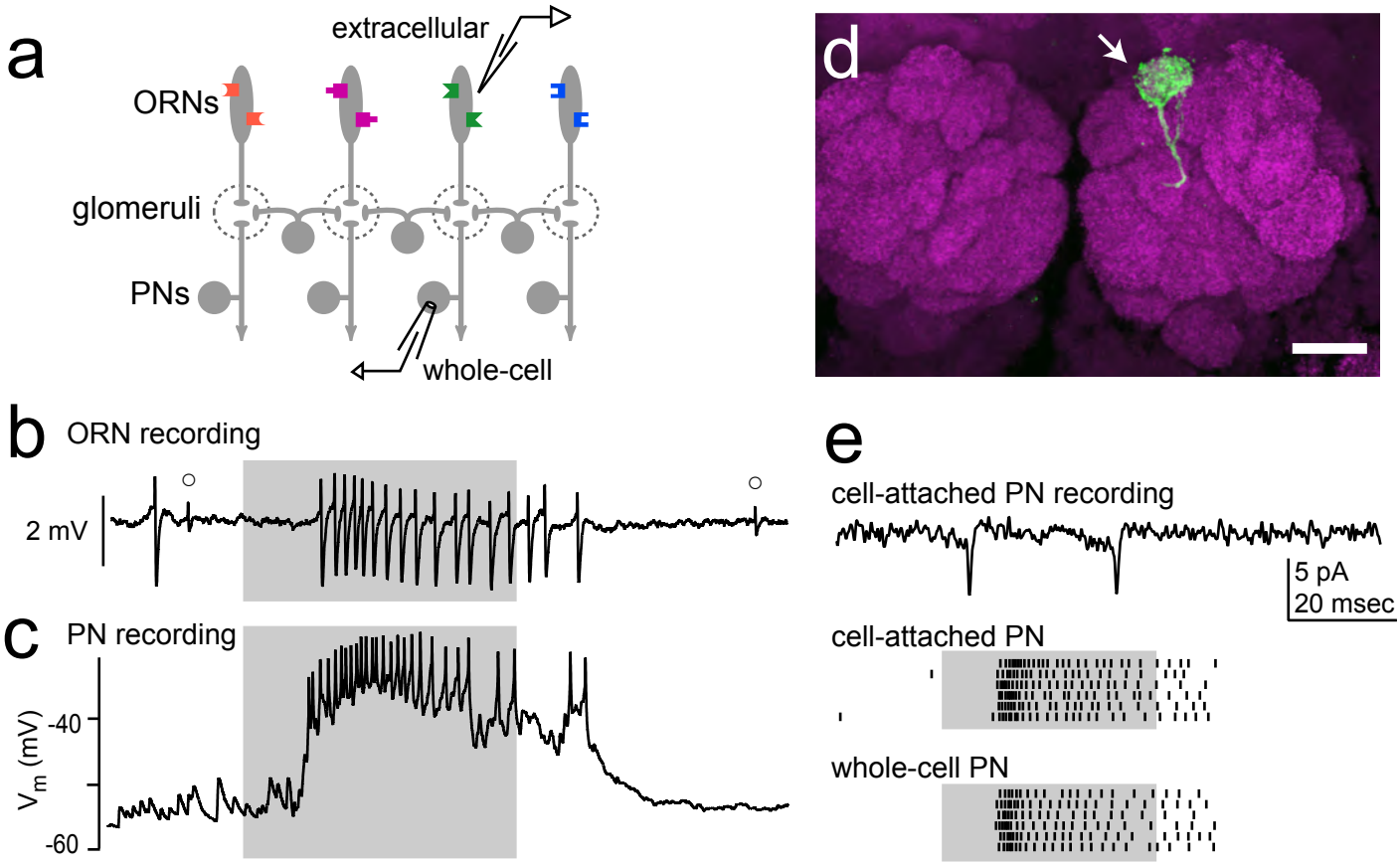

(a) All ORNs expressing the same receptor converge on the same glomerulus, where they make synapses with second-order PNs. Local interneurons interconnect glomeruli.
(b) Extracellular recording from a single antennal sensillum. Most sensilla contain the dendrites of two ORNs. In this example, the larger spikes are from an ORN that projects to glomerulus DM4. Smaller spikes (○) are from an ORN that projects to another glomerulus. Gray bar indicates the 500-ms period of odor delivery (ethyl butyrate).
(c) Whole-cell patch clamp recording from a PN in glomerulus DM4. Note spontaneous EPSPs. Odor (1-butanol) evokes a train of spikes.
(d) Projection of a confocal stack through the antennal lobes. Biocytin (green) labels the primary neurite of a PN whose dendritic tuft (arrow) terminates in glomerulus DM3. The soma and axon of this cell are not in this stack. Neuropil is labeled with nc82 antibody (magenta). Scale bar = 20 μm.
(e) Top: PN spikes recorded in cell-attached mode. Bottom: rasters show that an odor (ethyl butyrate) evokes a similar spike train in the same PN in cell-attached and whole-cell mode. These whole-cell responses were recorded 20 min. after break-in.

Supplementary Figure 2, part 1: Peri-stimulus time histograms

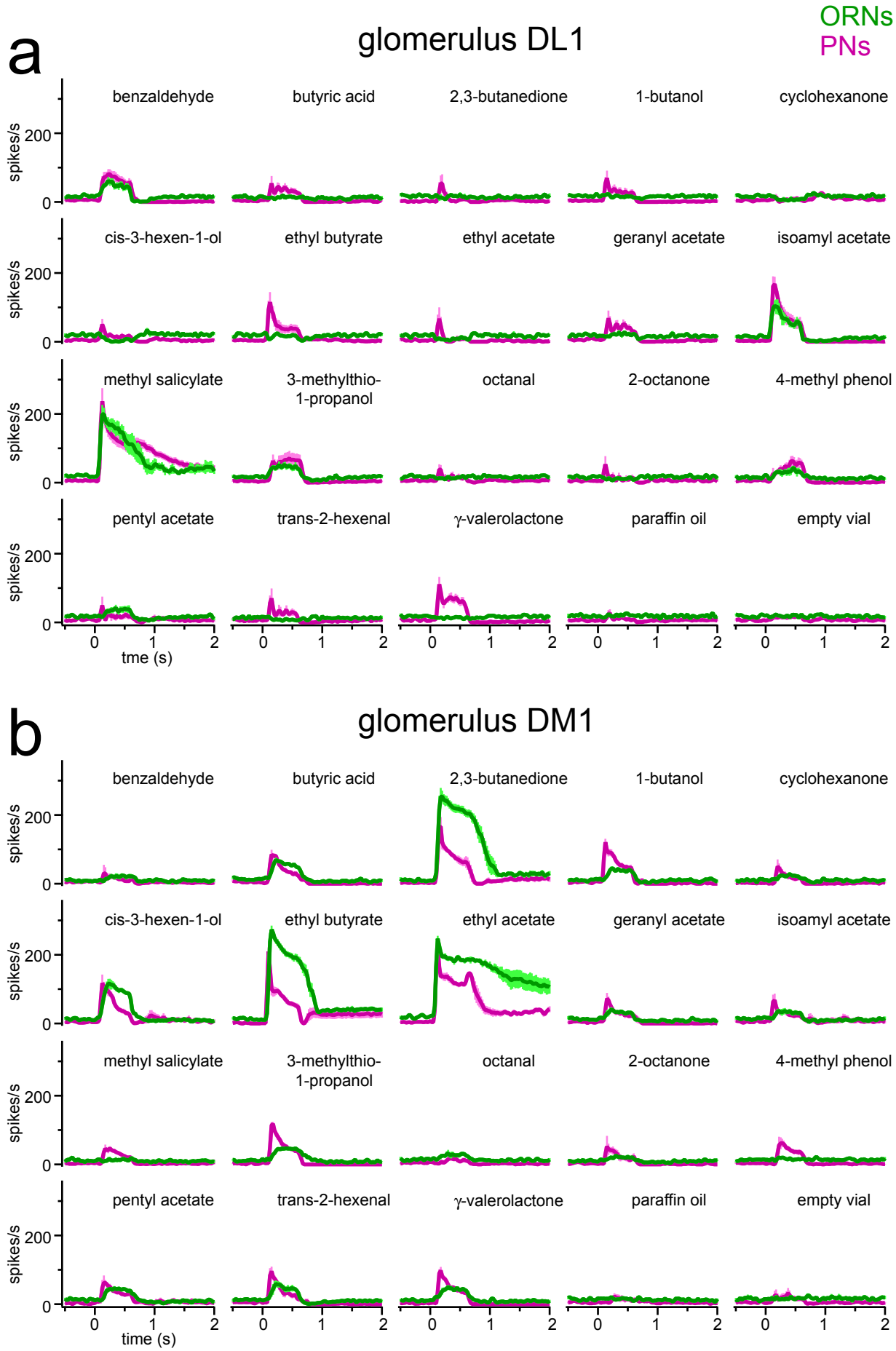

Supplementary Figure 2, part 2: Peri-stimulus time histograms

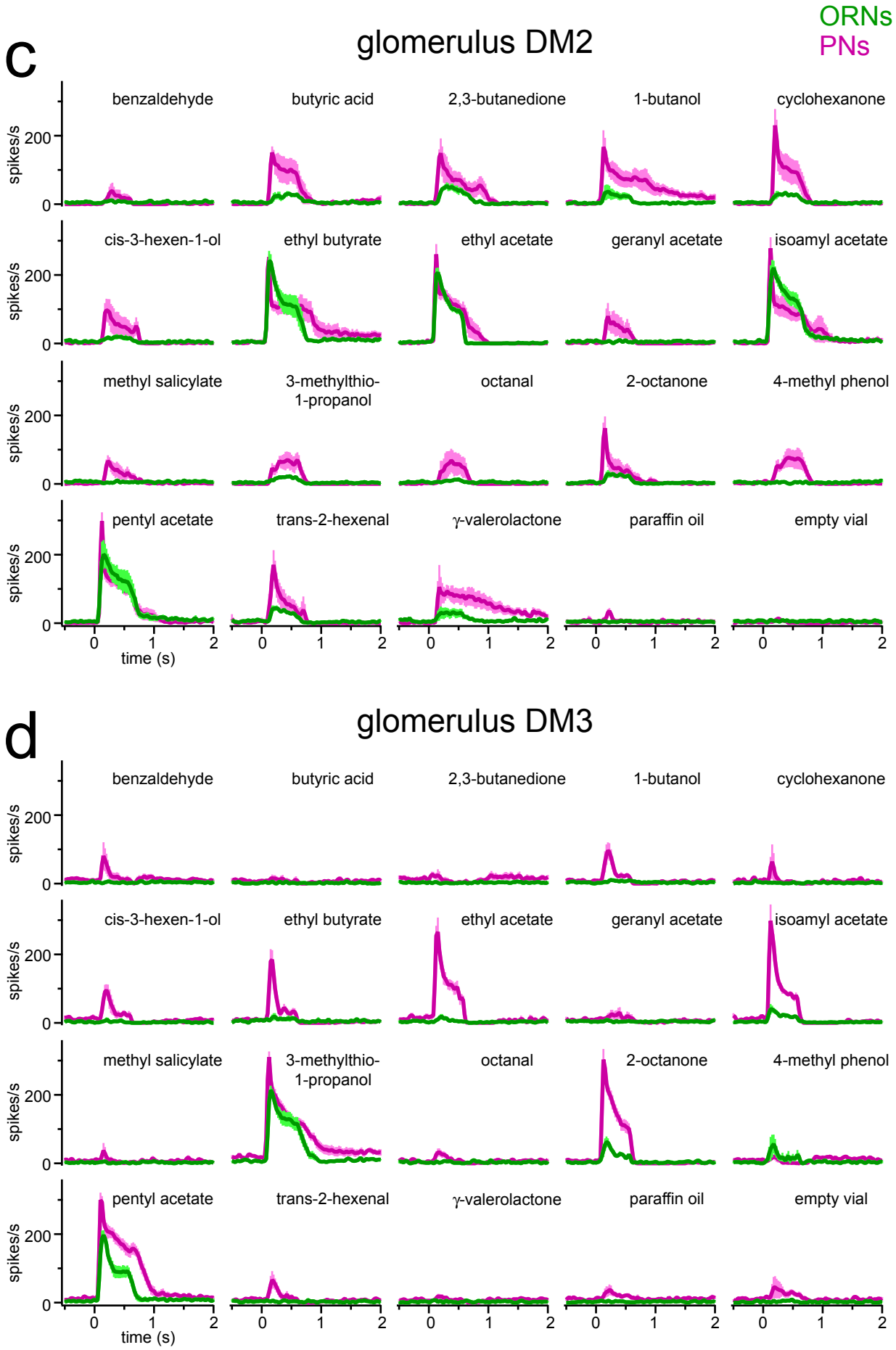

Supplementary Figure 2, part 3: Peri-stimulus time histograms

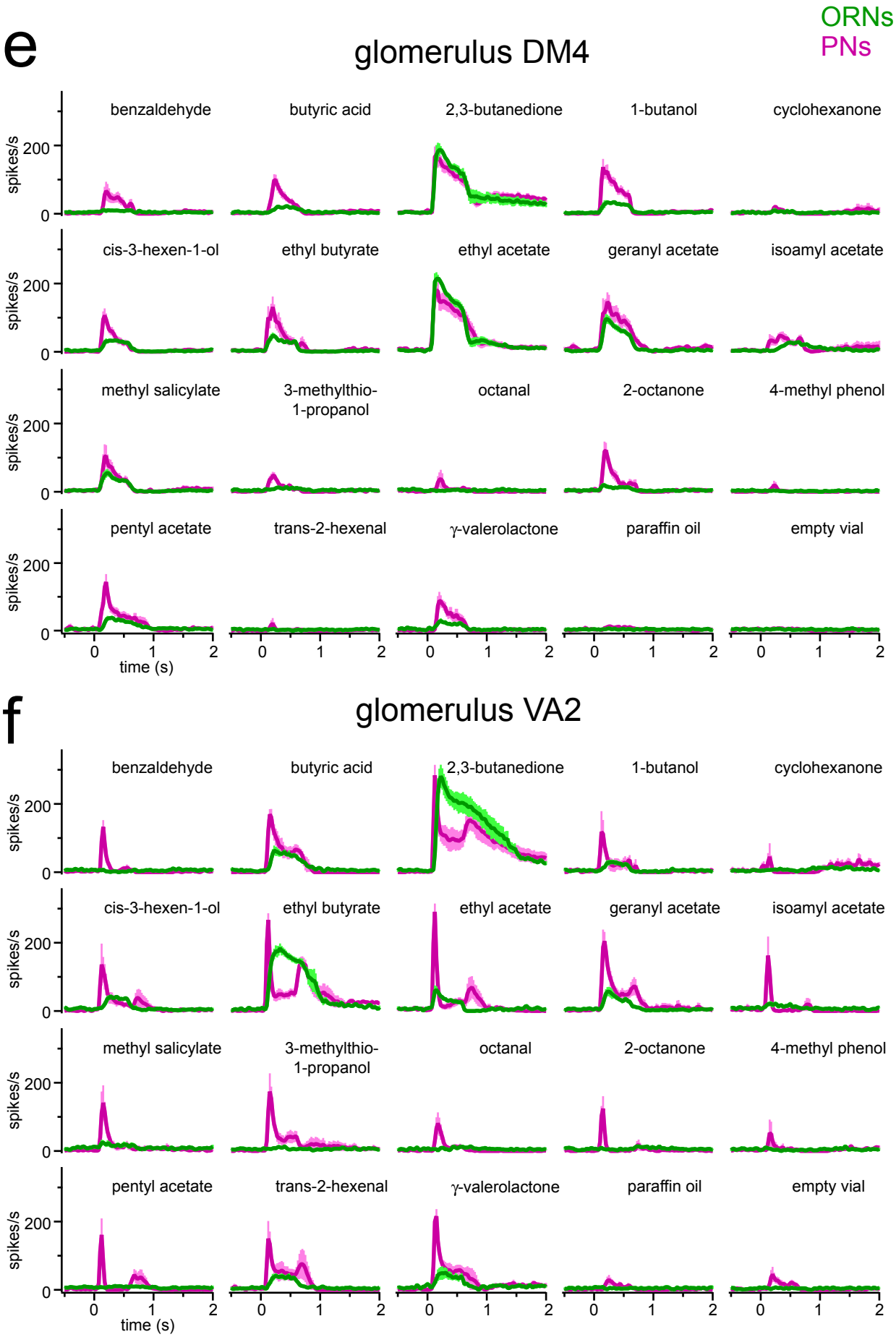

Supplementary Figure 2, part 4: Peri-stimulus time histograms

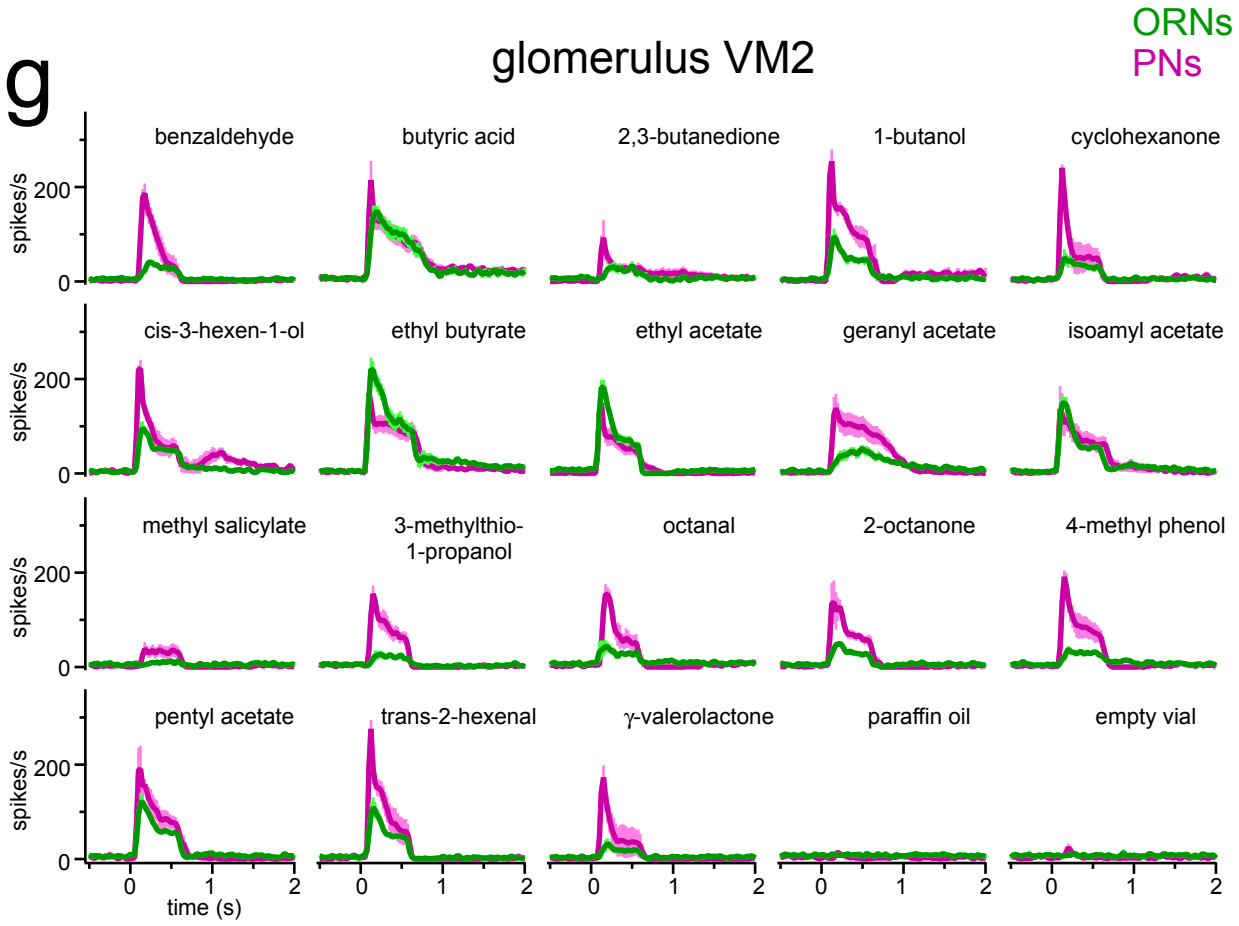

Mean PSTHs (± s.e.m) averaged across experiments for ORNs (green) and PNs (magenta) corresponding to seven glomeruli. The odor stimulus in each panel is from 0.0 to 0.5 seconds. All panels use the same *x*- and *y*-axes. Spike counts are computed in 50-msec bins overlapping by 25 msec. Baseline firing rates were not subtracted from the data displayed in this figure. See Supplementary Table 2 for the number of replicates corresponding to each panel.

Supplementary Figure 3: ORNs and PNs differ in their average odor response profiles (measured over the entire stimulus period)

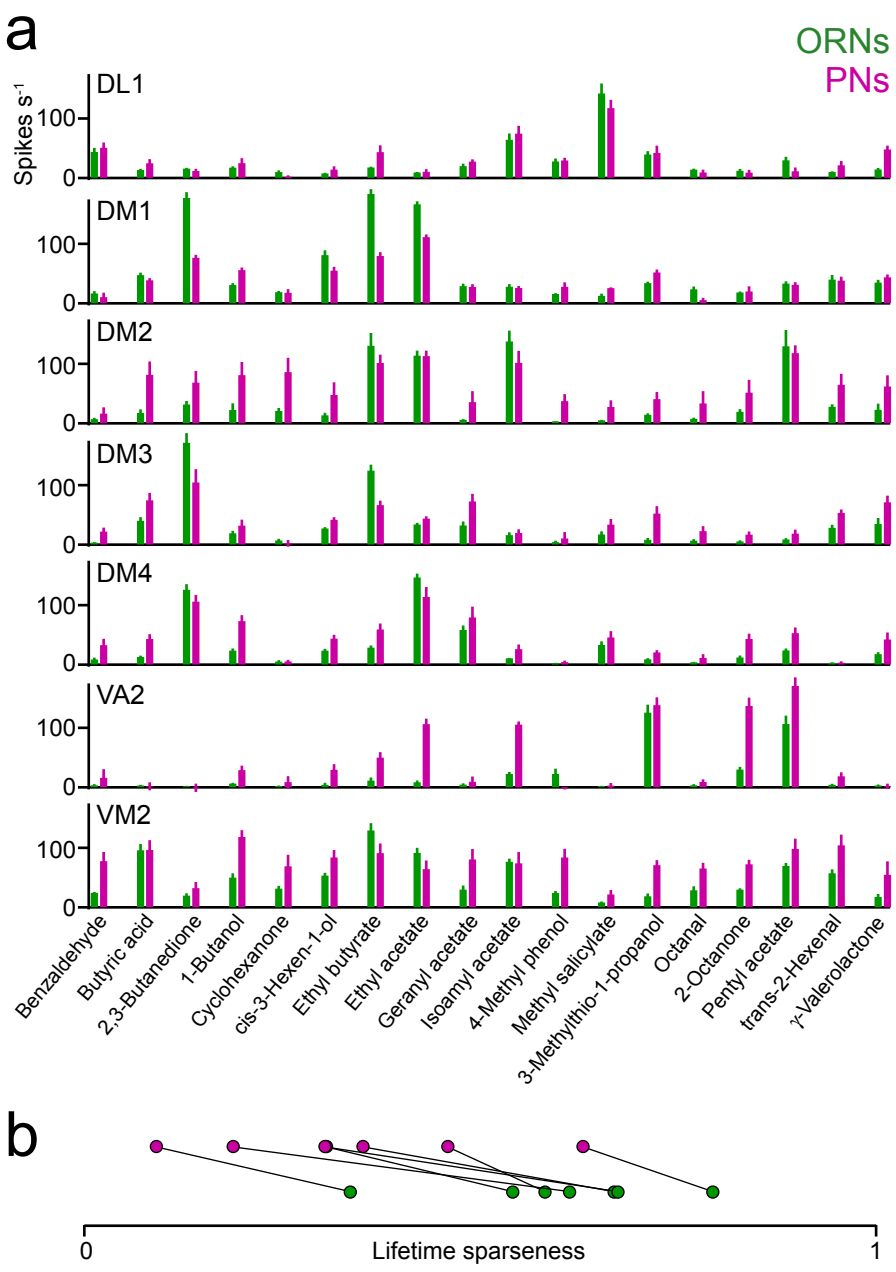

This figure is identical to Fig. 3, except that responses are calculated over the entire 500-ms odor stimulus period. As in Fig. 3, baseline firing rate is subtracted from each response.

(a) Response profiles for 7 ORN types (green) and 7 PN types (magenta) corresponding to the same glomeruli. Bars show averages across all experiments (± s.e.m., see Supplementary Table 2 for number of replicates).
(b) The selectivity of each response profile is quantified as lifetime sparseness (0 = unselective, 1 = maximally selective). ORNs and PNs corresponding to the same glomeruli are connected. PNs are consistently less selective than their corresponding ORNs.

Supplementary Figure 4: ORN and PN peri-stimulus time histograms at different odor concentrations

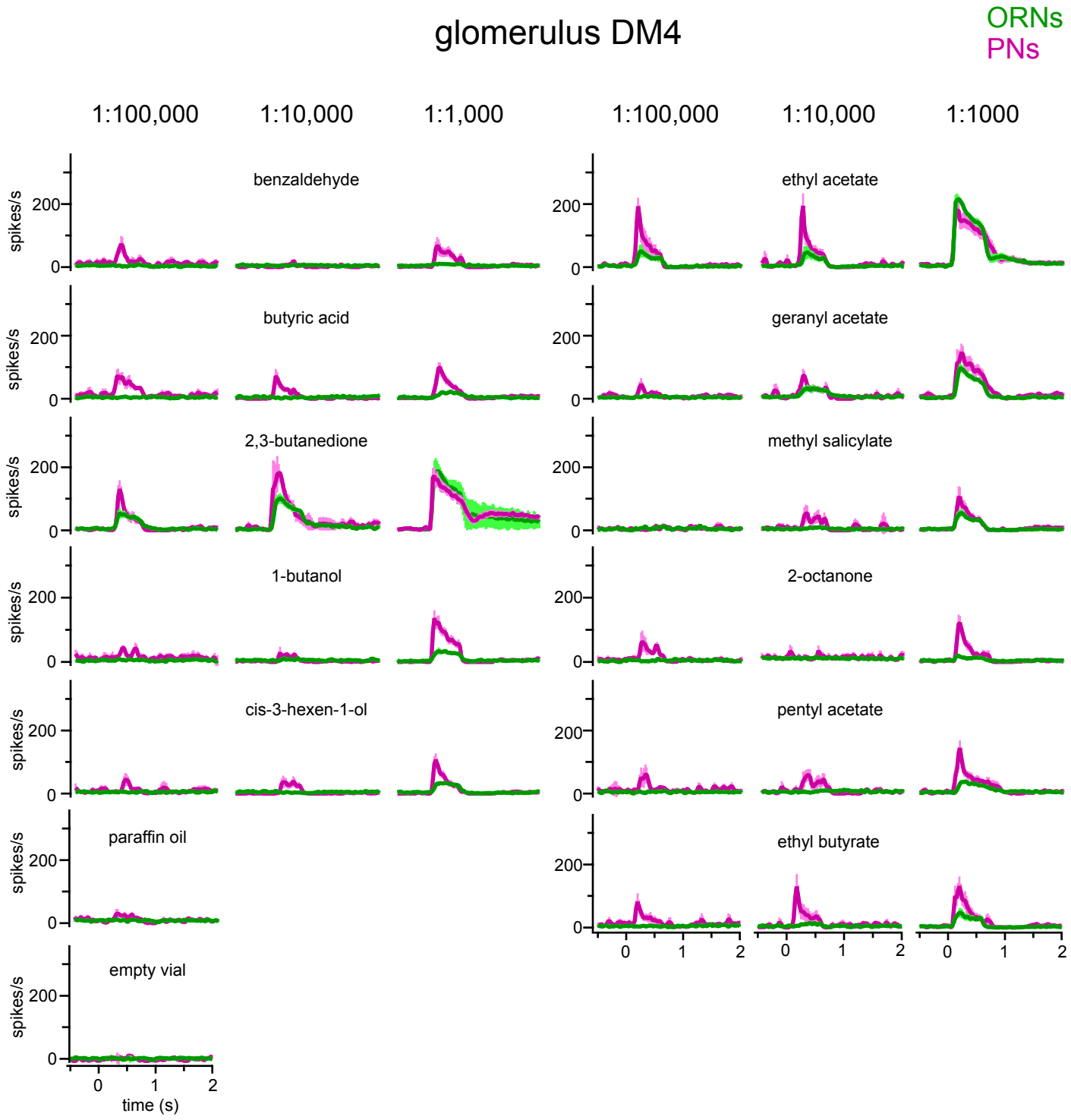

Mean PSTHs (± s.e.m) averaged across experiments for ORNs (green) and PNs (magenta) corresponding to glomerulus DM4. Eleven odor stimuli are presented at three different dilutions. PSTHs showing responses to the strongest stimulus (1:1,000 dilution) are the same as in Supplementary Figure 2e. Note that for a few odors, the PN response is larger for the lowest concentration (1:100,000) as compared to an intermediate concentration (1:10,000). This finding was consistent across experiments.

The odor stimulus in each panel is from 0.0 to 0.5 seconds. All panels use the same *x*- and *y*-axes. Spike counts are computed in 50-msec bins overlapping by 25 msec. Baseline firing rates were not subtracted from the data displayed in this figure. See Supplementary Table 3 for the number of replicates corresponding to each panel.

Supplementary Figure 5: PN odor responses are partly explained by a highly nonlinear transformation of their direct ORN inputs (measured over the entire stimulus period)

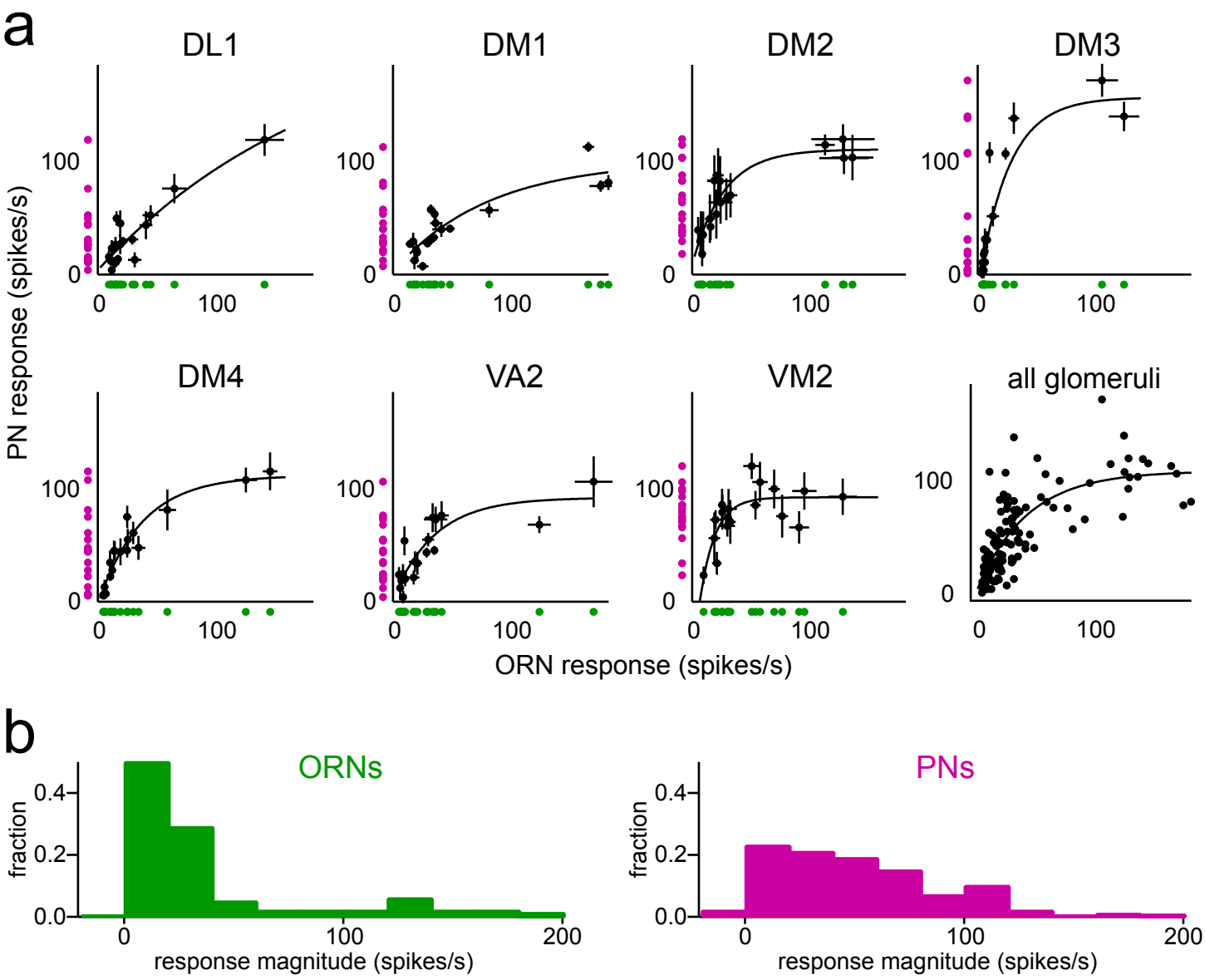

This figure is identical to Fig. 6, except that responses are calculated over the entire 500-ms odor stimulus period. As in Fig. 6, baseline firing rates are not subtracted from each response magnitude.

(a) For each glomerulus, average PN response to an odor is plotted versus the average ORN response to that odor (black symbols, ± s.e.m.). Curves are exponential fits ($y=y_0+A \cdot e^{kx}$). Green and magenta points are projections of the data onto the *x*- and *y*-axes, showing that odor responses generally occupy a PN's dynamic range more evenly than they occupy an ORN's dynamic range.
(b) Histograms of ORN and PN response magnitudes. Each histogram is accumulated across all 126 response magnitudes (= 7 glomeruli ×18 odors). The PN histogram is flatter than the ORN histogram, indicating that PNs use their dynamic range more efficiently.

Supplementary Figure 6: Correlations between different glomeruli are similar for ORNs and PNs (measured over the entire stimulus period)

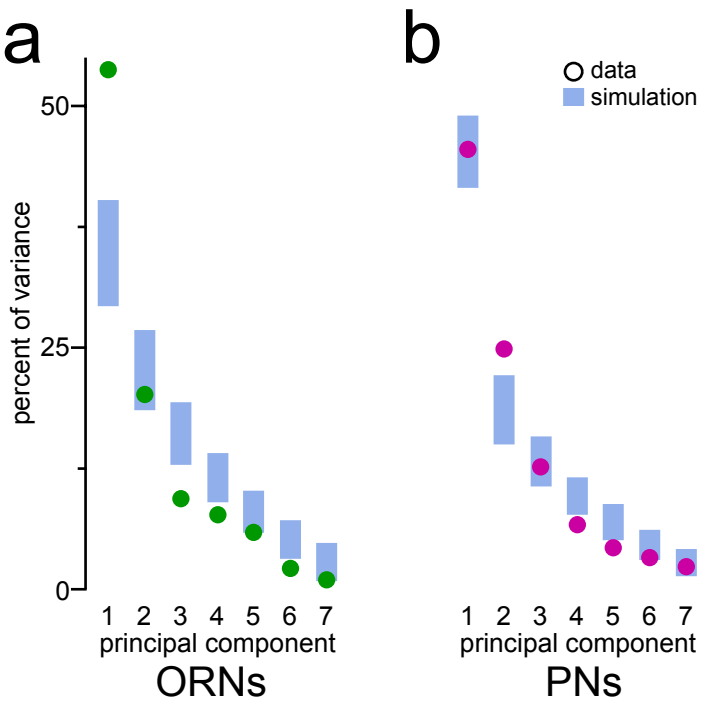

This figure is identical to Fig. 8, except that responses are calculated over the entire 500-ms odor stimulus period.

(a) Principal components analysis (PCA) was applied to the 18×7 ORN response matrix. The magnitude of the variance accounted for by each PC (green circles) is a measure of the correlations between different ORN types. Blue bands indicate the range of results obtained by shuffling odor labels on each glomerular response profile (see Methods). Comparison between data and simulation shows that ORNs are less independent in their odor responses than we would expect based simply on the distribution of response magnitudes within each glomerular coding channel.
(b) Same as (a) for the 18×7 PN response matrix. Correlations between PN types are similar to correlations between ORN types, although there is a trend toward decorrelation.

Fly stocks

Fly stocks were kindly provided as follows: *NP3529-Gal4*, *NP5221-Gal4*, *NP5103-Gal4*, and *NP3062-Gal4* (Kei Ito and Liqun Luo); *GH146-Gal4* (Liqun Luo); *Or42b-Gal4*, *Or92a-Gal4*, and *Or22a-Gal4* (Leslie Vosshall); *UAS-DTl/CyO* and *UAS-DTl$_{III}$* (Leslie Stevens). *UAS-CD8GFP$_{I}$, UAS-CD8GFP$_{II}$, UAS-CD8GFP$_{III}$* , *UAS-GFP.nls$_{III}$* ,and *Or42b[EY14886]* were obtained from the Bloomington Stock Center.

ORN recordings

Recorded ORNs were matched with a glomerulus based on: (1) sensillum morphology and size, (2) sensillum position on the antenna, (3) spike amplitude, (4) spontaneous spike frequency, and (5) odor tuning of cells in a sensillum. Because all these properties are a stereotyped function of cell lineage, together they form an unambiguous signature of ORN identity[1, 2]. To sort spikes accurately from some ORN types, it was necessary to kill a different ORN type in the same sensillum using diphtheria toxin (See Supplementary Table 4).

PN recordings

The composition of the internal patch-pipette solution was (in mM): potassium aspartate 140, HEPES 10, MgATP 4, Na_3GTP 0.5, EGTA 1, KCl 1, biocytin hydrazide 13 (pH = 7.3, osmolarity adjusted to ~ 265 mOsm). We found that PN odor responses are similar in cell-attached and whole-cell mode, demonstrating that intracellular dialysis does not affect PN receptive fields (Supplementary Fig. 1). The composition of the external saline solution was (in mM): NaCl 103, KCl 3, *N*-tris(hydroxymethyl) methyl-2-aminoethane-sulfonic acid 5, trehalose 8, glucose 10, $NaHCO_3$ 26, NaH_2PO_4 1, $CaCl_2$ 1.5, and $MgCl_2$ 4. Osmolarity was adjusted to 270–275 mOsm. The saline was bubbled with 95% O_2/5% CO_2 and reached a final pH = 7.3. Recordings were obtained with an A-M Systems Model 2400 amplifier in the current clamp mode (10MΩ headstage), low-pass filtered at 5 kHz, and digitized at 10 kHz. Data was acquired in Igor Pro. An Olympus BX51WI microscope with a 40x water-immersion objective and IR-DIC optics was used to obtain recordings under visual control. Each recorded PN was visualized with biocytin-streptavidin and nc82 histochemistry. All recorded PNs had a dendrite in a single glomerulus. The nc82 antibody was obtained from the Developmental Studies Hybridoma Bank (U. of Iowa). Glomeruli were identified using published maps[3, 5]. PNs were randomly selected among

GFP-positive somata in *GH146-Gal4,UAS-CD8GFP* flies, or in more specific enhancer trap lines (see Supplementary Table 4). We observed that a given PN type had similar odor responses in all the genotypes we tested, except that we found two types of DL1 PNs in *NP3529-Gal4,UAS-nlsGFP* flies: four PNs whose odor responses were distinctly weak, and eight PNs whose responses were very similar to the nine DL1 PNs we recorded in *GH146-Gal4,UAS-CD8GFP* flies. All of these DL1 PNs had similar morphologies. We omitted the four "weak" DL1 PNs from our analyses. Including them did not change any of our conclusions, but it decreased most of the average DL1 PN odor responses by 10–20%.

Olfactory stimulation

Odor dilutions were replaced with fresh dilutions every 10 days. A constant stream of charcoal-filtered air (2.2 L min^{-1}) was directed at the fly throughout each experiment. When triggered by a voltage pulse, a three-way solenoid valve redirected 10% of the airstream (0.22 L min^{-1}) through the headspace of the odor vial for 500 ms. Thus, all odors were diluted by an additional 10-fold factor just before reaching the fly. The odor stream rejoined the non-odor stream 16 cm from the end of the end of the delivery tube, which measured 3 mm in diameter and was positioned 8 mm from the fly. Odor presentations (typically 6 trials per odor) were spaced 40–60 sec apart, and responses to the first trial were excluded from our analysis. Odor details are at http://wilson.med.harvard.edu/odors.html. We do not know the absolute latency between the trigger pulse and the time the odor stimulus actually reaches the antennae, so all latencies in Fig. 2 represent the upper bound of the biological latency.

Data analysis

Spike times were extracted from raw ORN and PN recordings using routines in Igor Pro. Each cell was tested with multiple odors, and each odor was presented 6 times at intervals of 40–60 sec (a "block" of trials). The response to the first presentation was not included in our analysis. Each of the 5 remaining trials was converted into a peri-stimulus-time histogram (PSTH) by counting the number of spikes in 50-ms bins that overlapped by 25 ms. These single-trial PSTHs were averaged together to generate a PSTH describing the response to an odor in a given experiment. Multiple cells corresponding to each glomerular class and each cell

type (ORN or PN) were tested with a given odor in multiple experiments, each with a different fly. The *n* for each odor/cell-type combination are listed in Supplementary Tables 2 and 3. Average PSTHs in Fig. 2 and Supplementary Fig. 2 represent the mean ± s.e.m computed across experiments.

The CV of an odor response (Fig. 1) was computed separately for each block of 5 consecutive trials by dividing the SD by the mean for that block. If in a block of five trials there were zero spikes in a particular time bin, the CV was set to zero for that time bin.

In Fig. 2a, we normalized each of the PSTHs in Supplementary Fig. 2 to their peak, averaged them, and normalized the ORN and PN averages to the same peak. For the analyses in Fig. 2d, our starting point was the set of average PSTHs in Supplementary Fig. 2. We discarded any pair of PSTHs where either the ORN or the PN response failed to reach 20 spikes s^{-1} above baseline because small responses are noisy. (This was the only analysis where we discarded these responses.) Our data set then consisted of 69 pairs of PSTHs. We computed the latency to peak and time from peak to half-decay for each of these PSTHs, and then compared these values for ORNs and PNs using paired t-tests.

We quantified the selectivity of a neuron's odor response profile (Fig. 3, Fig. 4, Supplementary Fig. 3) by computing lifetime sparseness[3, 4]:

$$S = \frac{1}{1-1/N}\left(1-\frac{\left(\sum_{j=1}^{N} r_j / N\right)^2}{\sum_{j=1}^{N} r_j{}^2 / N}\right)$$

where N=number of odors, and r_j is the analog response intensity of the neuron to odor j, minus baseline firing rate. Analog response intensity was either the mean spike rate (averaged across experiments) during the entire 500-ms odor stimulus period (Supplementary Fig. 3), or mean spike rate (averaged across experiments) during a 100-ms window beginning 100 ms after odor stimulus onset (Fig. 3). Any values of r_j <0 were set to zero before computing lifetime sparseness. (This was the only analysis in this study where negative responses were zeroed.)

In Fig. 5, we created two simulated individual ORN response profiles and two simulated PN response profiles for each glomerulus by randomly sampling from a normal distribution described by the mean and

standard deviation (SD) of the average response profile. Next, we calculated the Spearman rank correlation coefficient (r_s) on the odor ranks of the two simulated ORN profiles, the two simulated PN profiles, and for each of the four ORN/PN combinations. This procedure was repeated 2000 times for each glomerular class, and the distributions of r_s were accumulated from all glomerular classes (Fig. 5b). If variability between experiments was the sole explanation for the difference in ORN and PN odor ranks, then the distribution of ORN/PN correlations should be intermediate between the ORN/ORN correlations and the PN/PN correlations. This is because when we sample from one distribution with a small SD (simulated ORN profiles) and one with a larger SD (simulated PN profiles), the combined variability affecting r_s should be smaller than when we sample twice from the distribution with larger SD (i.e., when we pick two simulated PN tuning curves).

PCA (Fig. 7a-b and Fig. 8) was performed in IgorPro on the 18×7 odor response matrix, where response magnitudes are expressed as firing rate increases or decreases versus baseline during the 100-ms period when firing rates are peaking (as in Fig. 3). (Supplementary Fig. 6 shows the same analysis where response magnitudes are expressed as firing rate increases or decreases versus baseline during the entire 500-ms odor stimulus period.) The average response magnitude for each glomerular column was subtracted from that column before performing PCA. PCA was performed separately on ORN and PN data. Euclidean distances were measured in the full 7-glomerular space prior to dimensionality reduction with PCA.

Simulations (Figs. 7 and 8 and Supplementary Fig. 6) assessed how the distribution of response magnitudes for each cell type affected inter-odor distances and inter-glomerulus correlations. For each glomerular class, we randomly and independently permuted the list of our 18 test odors, and attached this list to the average response vector associated with that glomerular type. Thus, the odor preferences for each glomerulus were made independent from each other. An ORN type and PN type corresponding to the same glomerulus were associated with the same odor list. For Fig. 7c,d we used this simulated data to compute the median and inter-quartile range of all pair-wise inter-odor distances. We performed 200 runs of the simulation, and accumulated a distribution of results. Blue bands represent the ranges that contain the central 95% of these distributions. For Fig. 8 (and Supplementary Fig. 6) we performed PCA on each simulated data set and

computed the variance associated with each PC. We performed 1000 runs of the simulation for this analysis. Blue bands represent the ranges that contain the central 95% of the distribution of simulated variances.

Linear discriminant analysis (Fig. 9) was performed using the lda() function of the MASS package[5] in R 2.5.0[6]. Individual cells from each of the 7 glomerular classes were chosen for each of the 18 odors analyzed. For each odor, five spike trains were selected from each cell and randomly matched with spike trains of the cells of the other glomerular classes. Therefore, each data set contained 90 "ensemble responses." Spike trains were represented as spike counts in 50 ms bins that overlap by 25 ms. To estimate the classification success rate for every time bin, each "ensemble response" was classified using the leave-one-out cross-validation method built into the lda() function. That is, a single "ensemble response" was omitted from the training data set, discriminant functions were generated on the basis of 89 “ensemble responses”, and then the holdout “ensemble response” to one odor was classified using the discriminants generated by the analysis. This was done for each of the 90 "ensemble responses" in every time bin., and the average success rate was computed as the number of correct classifications divided by the total number of classifications. A uniform distribution of prior probabilities was used in the analysis. Points in Fig. 9 represent mean ± s.e.m., averaged across twenty repetitions of the entire procedure.

Non-parametric statistics (Mann-Whitney U test, Wilcoxon signed rank test, Spearman’s rank correlation coefficient) were computed in R 2.5.0[6].

References

1. de Bruyne, M., Clyne, P. J. & Carlson, J. R. Odor coding in a model olfactory organ: the Drosophila maxillary palp. J. Neurosci. 19, 4520-32 (1999).
2. de Bruyne, M., Foster, K. & Carlson, J. R. Odor coding in the Drosophila antenna. Neuron 30, 537-52 (2001).
3. Vinje, W. E. & Gallant, J. L. Sparse coding and decorrelation in primary visual cortex during natural vision. Science 287, 1273-6 (2000).
4. Perez-Orive, J. et al. Oscillations and sparsening of odor representations in the mushroom body. Science 297, 359-65 (2002).
5. Venables, W. N. & Ripley, B. D. Modern Applied Statistics with S. (Springer, New York, 2002).
6. Ihaka, R. & Gentleman, R. R: A Language for Data Analysis and Graphics. Journal of Computational and Graphical Statistics 5, 299-314 (1996).

Supplementary Table 1: Linear correlations between ORN and PN odor responses (Pearson's r^2).

	DL1	DM1	DM2	DM3	DM4	VA2	VM2
correlation between ORNs and PNs	0.81	0.76	0.70	0.60	0.78	0.58	0.26
correlation between cells of the same type	0.88	0.93	0.74	0.94	0.84	0.85	0.62

First row: Correlation between the average ORN response profile and the average PN response profile for each glomerulus. Responses were quantified as firing rates over the 500-msec odor stimulus period. All seven correlations are significant ($p<0.05$; similar results were obtained for the 100ms epoch at the peak of the response, except the correlation between VM2 ORNs and PNs did not reach statistical significance during this epoch).
Second row: Average correlation between different ORNs of the same type or different PNs of the same type, recorded in different experiments. These values are significantly higher than the correlations in the first row ($p<0.05$, paired t-test, $n=7$ glomeruli; similar results were obtained for the 100ms epoch at the peak of the response). To obtain these values, we randomly divided all cells belonging to the same type into two groups. We then computed average tuning curves for each group and computed the correlation coefficient r between the two halves. We repeated this procedure 20 times for each ORN type and 20 times for each PN type, averaged together the r values from all 40 runs, and squared this to obtain r^2.

Supplementary Table 2: Number of replicates (n) for each odor/cell type combination.

	DL1		DM1		DM2		DM3		DM4		VA2		VM2	
	ORNs	PNs	ORNs	PNs	ORNs	PNs	ORNs	PNs	ORNs	PNs	ORNs	PNs	ORNs	PNs
benzaldehyde	5	12	4	5	6	4	5	8	10	9	5	5	5	5
butyric acid	4	7	5	6	4	4	4	5	9	9	5	4	6	9
2,3-butanedione	4	5	5	5	6	4	5	5	11	11	5	5	4	6
1-butanol	6	9	5	6	6	5	5	6	9	11	4	4	5	4
cyclohexanone	5	11	4	5	6	4	5	4	5	4	5	5	5	5
cis-3-hexen-1-ol	4	9	5	6	5	4	3	6	11	10	5	5	6	5
ethyl butyrate	4	10	5	6	6	4	4	6	12	8	4	6	6	10
ethyl acetate	4	5	4	5	5	4	5	4	13	9	4	5	8	8
geranyl acetate	4	6	5	6	5	4	10	5	11	9	5	5	6	9
isoamyl acetate	4	10	5	6	5	4	9	6	5	5	5	4	6	7
methyl salicylate	5	13	5	5	7	4	4	5	12	9	5	4	4	7
3-methylthio-1-propanol	8	10	5	6	7	4	11	7	5	5	5	5	5	6
octanal	5	10	4	6	5	4	3	6	5	5	4	5	5	4
2-octanone	5	7	5	6	7	5	5	6	11	10	5	5	6	4
4-methyl phenol	4	6	6	5	4	4	3	5	6	5	4	5	6	5
pentyl acetate	5	9	7	6	4	6	10	6	9	11	6	5	6	5
trans-2-hexenal	4	8	5	6	6	4	4	6	5	5	5	5	6	4
γ-valerolactone	5	6	5	6	4	4	3	6	5	5	4	5	6	4
paraffin oil	4	10	4	5	7	4	5	5	6	4	4	5	5	6
empty vial	5	8	4	6	6	4	4	5	6	4	4	5	5	5

Replicates for ORNs are numbers of single-sensillum recordings (generally 1-2 per fly). Replicates for PNs are numbers of whole-cell recordings (1 per fly). Each replicate consists of 5 presentations of the same odor (a "block of trials").

Supplementary Table 3: Number of replicates (n) for odor dilution experiments with glomerulus DM4.

	1:1,000		1:10,000		1:100,000	
	ORNs	PNs	ORNs	PNs	ORNs	PNs
benzaldehyde	10	9	7	5	4	5
butyric acid	9	9	6	5	4	7
2,3-butanedione	11	11	6	5	4	7
1-butanol	9	11	6	5	4	7
cis-3-hexen-1-ol	11	10	6	5	5	7
ethyl butyrate	12	8	6	6	4	5
ethyl acetate	13	9	5	5	5	5
geranyl acetate	11	9	6	5	6	5
methyl salicylate	12	9	5	6	5	5
2-octanone	11	10	5	5	4	5
pentyl acetate	9	11	5	5	4	5

Replicates for ORNs are numbers of single-sensillum recordings (generally 1-2 per fly). Replicates for PNs are numbers of whole-cell recordings (1 per fly). Each replicate consists of 5 presentations of the same odor (a "block of trials"). Experiments at the highest concentration (1:1,000) are the same experiments as in Supplementary Table 2.

Supplementary Table 4: Genotypes used in each type of recording.

DL1	ORNs	*w[1118]* or *Or42b[EY14886]*[a] **or** *Or42b-Gal4/UAS-DTl;Or92a-Gal4/UAS-DTl*[b]
	PNs	*GH146-Gal4,UAS-CD8GFP*[c] **or** *NP3529-Gal4,UAS-GFP.nls*[d]
DM1	ORNs	*UAS-DTl/CyO;Or92a-Gal4*[e]
	PNs	*NP5221-Gal4,UAS-CD8GFP*[f]
DM2	ORNs	*GH146-Gal4,UAS-CD8GFP*[c] **or** *Or22a-Gal4,UAS-CD8GFP*[g]
	PNs	*GH146-Gal4,UAS-CD8GFP*[c] **or** *Or22a-Gal4,UAS-CD8GFP*[g]
DM3	ORNs	*GH146-Gal4,UAS-CD8GFP*[c] **or** *w[1118]* **or** *Or82a-Gal4;UAS-DTl*[h]
	PNs	*GH146-Gal4,UAS-CD8GFP*[c]
DM4	ORNs	*GH146-Gal4,UAS-CD8GFP*[c] **or** *NP3481-Gal4,UAS-CD8GFP*
	PNs	*GH146-Gal4,UAS-CD8GFP*[c] **or** *NP3062-Gal4,UAS-CD8GFP*[i]
VA2	ORNs	*Or42b[EY14886]*[a] **or** *Or42b-Gal4;UAS-DTl*[j]
	PNs	*GH146-Gal4,UAS-CD8GFP*[c]
VM2	ORNs	*GH146-Gal4,UAS-CD8GFP*[c] **or** *w[1118]*
	PNs	*GH146-Gal4,UAS-CD8GFP*[c] **or** *NP5103-Gal4,UAS-CD8GFP*[k]

[a] pBac insertion in the *Or42b* gene (Bloomington Stock Center). We have observed that this mutation abolishes odor responses in ab1A ORNs, allowing us to count more accurately the spikes from ab1D (DL1) and ab1B(VA2) ORNs in response to odors that normally drive the ab1A ORNs strongly.

[b] In some experiments we killed ab1A and ab1B ORNs by expressing diphtheria toxin selectively in these cells. This allowed us to more accurately detect the small spikes of ab1D (DL1) ORNs in response to odors that normally drive both either the ab1A or ab1B ORNs strongly.

[c] The *GH146-Gal4* enhancer trap line drives Gal4 expression in a large subset of PNs (Stocker et al., 1997).

[d] The *NP3529-Gal4* enhancer trap line drives Gal4 expression selectively in DL1 PNs (Tanaka et al., 2004).

[e] In some experiments we killed ab1B ORNs by expressing diphtheria toxin selectively in these cells, allowing us to count more accurately the spikes from ab1A (DM1) ORNs.

[f] The *NP5221-Gal4* enhancer trap line drives Gal4 expression in DM1 PNs, in addition to VA4 PNs and VC1 PNs (Liqun Luo, personal communication), and VC2 PNs (S.R.O, unpublished observations).

[g] *Or22a-Gal4,UAS-CD8GFP* drives GFP expression intensely in the DM2 ORNs. We used this line in some experiments to cross-check our identification of DM2 ORNs based on odor tuning and sensillum position. We also recorded from two DM2 PNs in this genotype, and in both cases verified that the biocytin-filled dendritic tuft of these PNs co-localized with CD8-immunoreactive ORN axon terminals.

[h] In some experiments we killed ab5A neurons by expressing diphtheria toxin selectively in these cells, allowing us to count more accurately the spikes from ab5B (DM3) ORNs.

[i] The *NP3062-Gal4* enhancer trap line drives Gal4 expression in DM4 PNs, in addition to DM6 PNs (Liqun Luo, personal communication, and V.B. unpublished observations).

[j] In some experiments we killed ab1A neurons by expressing diphtheria toxin selectively in these cells, allowing us to count more accurately the spikes from ab1B (VA2) ORNs.

[k] The *NP5103-Gal4* enhancer trap line drives Gal4 expression selectively in VM2 PNs (Tanaka et al., 2004).